

Single neutron transfer coupling effects on sub-barrier elastic scattering and near-barrier fusion of ^{15}C

N. Keeley* and N. Alamanos

*CEA/DSM/DAPNIA/SPhN Saclay,
91191 Gif-sur-Yvette Cedex, France*

(Dated: February 21, 2007)

Abstract

To date, the possible effects of coupling to nucleon transfer reactions on the elastic scattering and fusion of weakly bound exotic nuclei have been largely neglected. The ^{15}C nucleus presents a virtually unique opportunity to test these effects for an almost pure $s_{1/2}$ single neutron halo nucleus. We present a series of coupled reaction channels calculations of the sub-barrier elastic scattering and single neutron transfer reactions, plus near-barrier excitation functions of the total fusion cross section for the ^{12}C , ^{13}C and $^{15}\text{C} + ^{208}\text{Pb}$ systems. The method is validated against data for ^{12}C and $^{13}\text{C} + ^{208}\text{Pb}$. A large effect on the sub-barrier elastic scattering due to coupling to the $(^{15}\text{C}, ^{14}\text{C})$ single neutron stripping reaction is found, ascribed to the $2s_{1/2}$ halo nature of the ^{15}C ground state, in contrast to the two stable Carbon isotopes. We also find a significant diminution of the above barrier total fusion cross section for ^{15}C due to this coupling, again in contrast to the stable isotopes.

PACS numbers: 25.70.Bc, 25.70.Hi, 25.70.Jj, 24.10.Eq

*Electronic address: nkeeley@cea.fr; Permanent address: Department of Nuclear Reactions, The Andrzej Sołtan Institute for Nuclear Studies, Hoża 69, PL-00681, Warsaw, Poland

The elastic scattering of light exotic nuclei from heavy targets at energies close to the Coulomb barrier — and in this context we shall take “heavy” to mean nuclei of mass number greater than about 50 — has until recently been a rather neglected aspect of direct reaction studies. However, due to steady improvements in the quality of available radioactive beams and detector arrays it is now possible to measure elastic scattering angular distributions in this energy regime with good angular coverage and precision, see e.g. [1–3]. As most of the light exotic nuclei studied so far are weakly bound, interpretation of the available elastic scattering data has concentrated on the effect of coupling to breakup, see e.g. [4–7]. However, weak binding may also imply important effects due to nucleon transfer reactions, particularly for those weakly bound exotic nuclei that exhibit the halo phenomenon. Indeed, recent exclusive measurements for the ${}^6\text{He} + {}^{209}\text{Bi}$ system [8, 9] found that the one and two neutron transfer processes together account for approximately 75 % of the observed total α yield at an incident energy of ~ 23 MeV, close to the Coulomb barrier, indicating that transfer processes are the dominant contribution to the total reaction cross section.

A large cross section for a particular reaction process does not necessarily imply an equally important effect on the elastic scattering, although it is certainly suggestive. We present here a study of the effect of coupling to single neutron transfers on the elastic scattering of ${}^{15}\text{C}$ from a ${}^{208}\text{Pb}$ target at sub-barrier energies, plus the near-barrier total fusion cross section excitation function. We chose this system as it avoids potential complications with two-step neutron transfer processes associated with two-neutron halo systems such as ${}^6\text{He}$ and ${}^{11}\text{Li}$ and allows comparison with two stable isotopes, ${}^{12}\text{C}$ and ${}^{13}\text{C}$, for which sub-barrier elastic scattering and transfer data from a ${}^{208}\text{Pb}$ target are available [10]. We do not investigate ${}^{14}\text{C}$ as it also has potential complications due to the two-step neutron transfer mechanism. In addition, ${}^{15}\text{C}$ is virtually unique in exhibiting an almost pure $2s_{1/2}$ single neutron halo ground state. While ${}^{11}\text{Be}$ also has a $1/2^+$ ground state dominated by the $2s_{1/2}$ neutron + ${}^{10}\text{Be}(0^+)$ configuration, the experimental spectroscopic factors for this configuration cluster around 0.8, whereas for the ${}^{15}\text{C}$ ground state the experimental values for the corresponding $2s_{1/2}$ neutron + ${}^{14}\text{C}(0^+)$ configuration cluster around 1.0, see e.g. [11]. Therefore, effects due to core excitation should be much less important for ${}^{15}\text{C}$ than for ${}^{11}\text{Be}$ and will be ignored here.

Having set out our rationale for studying the ${}^{15}\text{C} + {}^{208}\text{Pb}$ system, we shall consider the single neutron stripping and pickup reactions for the three systems ${}^{12}\text{C} + {}^{208}\text{Pb}$, ${}^{13}\text{C}$

TABLE I: Reaction Q-values and projectile overlap spectroscopic factors (C^2S) for the single neutron stripping and pickup reactions for the $^{12,13,15}\text{C} + ^{208}\text{Pb}$ systems.

Reaction	Q-value (MeV)	C^2S
$^{208}\text{Pb}(^{12}\text{C}, ^{11}\text{C})^{209}\text{Pb}$	-14.8	2.85 ^a
$^{208}\text{Pb}(^{12}\text{C}, ^{13}\text{C})^{207}\text{Pb}$	-2.4	0.61 ^a
$^{208}\text{Pb}(^{13}\text{C}, ^{12}\text{C})^{209}\text{Pb}$	-1.0	0.61 ^a
$^{208}\text{Pb}(^{13}\text{C}, ^{14}\text{C})^{207}\text{Pb}$	+0.81	1.73 ^a
$^{208}\text{Pb}(^{15}\text{C}, ^{14}\text{C})^{209}\text{Pb}$	+2.7	0.98 ^a
$^{208}\text{Pb}(^{15}\text{C}, ^{16}\text{C})^{207}\text{Pb}$	-3.1	0.60 ^b , 1.23 ^c

^aRef. [12]

^bRef. [13], $^{15}\text{C}(1/2^+):^{16}\text{C}$

^cRef. [13], $^{15}\text{C}(5/2^+):^{16}\text{C}$

+ ^{208}Pb and $^{15}\text{C} + ^{208}\text{Pb}$. The Q-values for these reactions are summarized in Table I. Spectroscopic factors for the $^{12}\text{C}:^{11}\text{C}$, $^{12}\text{C}:^{13}\text{C}$, $^{13}\text{C}:^{14}\text{C}$ and $^{15}\text{C}:^{14}\text{C}$ overlaps were taken from the shell model results presented in [12] while those for the $^{15}\text{C}:^{16}\text{C}$ overlap were taken from [13]. The n+C binding potentials were of Woods-Saxon form, with $R_0 = 1.25 \times A^{1/3}$ fm, $a = 0.65$ fm and a spin-orbit term with the same geometry and a depth of 6 MeV, the depth of the central part being adjusted to obtain the correct binding energy. The use of “standard” binding potential parameters for the halo nucleus ^{15}C is, of course, questionable. However, increasing the radius and/or the diffuseness of the binding potential will lead to larger calculated transfer cross sections and a larger coupling effect on other channels. Our calculations therefore represent in some sense a lower limit for the transfer coupling effect for ^{15}C . Transfers to the 0.0 MeV $9/2^+$, 0.78 MeV $11/2^+$, 1.42 MeV $15/2^-$, 1.57 MeV $5/2^+$, 2.03 MeV $1/2^+$, 2.49 MeV $7/2^+$ and 2.54 MeV $3/2^+$ states of ^{209}Pb and the 0.0 MeV $1/2^-$, 0.57 MeV $5/2^-$, 0.90 MeV $3/2^-$, 1.63 MeV $13/2^+$ and 2.34 MeV $7/2^-$ states of ^{207}Pb were considered. Spectroscopic factors and neutron binding potentials for the $^{208}\text{Pb}:^{209}\text{Pb}$ and $^{208}\text{Pb}:^{207}\text{Pb}$ overlaps were taken from the adiabatic model analysis of [14] and [10], respectively.

For the “bare” optical model potentials in the entrance and exit channels we used the systematics of Broglia and Winther [15] and Woods-Saxon wells with parameters: $W = 50$ MeV, $R_W = 1.0 \times (A_p^{1/3} + A_t^{1/3})$ fm, $a_W = 0.3$ fm for the real and imaginary parts, respectively. An “interior” imaginary potential was employed to simulate the ingoing-wave boundary condition [16], and we may thus equate the total absorption by the imaginary potentials to the total fusion cross section. The results of the calculations are insensitive to the details of the imaginary potential, provided that it remains of an “interior” nature. The calculations were performed using the code Fresco [17] and included the full complex remnant term and non-orthogonality correction.

Data for the elastic scattering of $^{12,13}\text{C}$ from a ^{208}Pb target plus the corresponding single neutron transfer reactions are available for an incident C energy of 54.07 MeV [10]. The nominal Coulomb barriers for the ^{12}C , ^{13}C and $^{15}\text{C} + ^{208}\text{Pb}$ systems, defined as the maximum of the combined bare real nuclear plus Coulomb potentials, are 58.1 MeV, 57.6 MeV and 56.8 MeV, respectively, although the barrier for $^{15}\text{C} + ^{208}\text{Pb}$ does not take account of the halo nature of ^{15}C and should therefore be somewhat lower in reality. This incident energy is thus well below the barrier for all three systems and most reaction channels should be classically closed. The two stable C isotopes provide a useful benchmark for the ^{15}C calculations: for ^{12}C one expects essentially no effect from coupling to the single neutron transfer reactions due to the large negative Q-values involved; conversely, for ^{15}C one might naively expect a significant effect from coupling to the ($^{15}\text{C}, ^{14}\text{C}$) transfer, even at such a low incident energy, due to the relatively large positive Q-value. On this basis, ^{13}C should exhibit behavior intermediate between ^{12}C and ^{15}C . Of course, reaction Q-values are not the sole criteria for determining whether a particular coupling will have an important effect on elastic scattering, and these naive expectations may be significantly modified by other considerations, e.g. spectroscopic factors. The data for the $^{12,13}\text{C} + ^{208}\text{Pb}$ systems also provide a valuable check of the physical reasonableness of our method.

In Fig. 1 we show the results of our calculations for the elastic scattering of ^{12}C , ^{13}C and $^{15}\text{C} + ^{208}\text{Pb}$ at incident C energies of 54.07 MeV. For the $^{12}\text{C} + ^{208}\text{Pb}$ system we see that the effect of transfer couplings is entirely negligible, as expected, and that the bare no coupling calculation provides a good description of the data. Note that the full curve plotted in Fig. 1(a) does not include coupling to the $^{208}\text{Pb}(^{12}\text{C}, ^{11}\text{C})$ single neutron stripping as it has no effect whatsoever on the elastic scattering and the cross sections for this reaction are too

FIG. 1: Elastic scattering for $^{12}\text{C} + ^{208}\text{Pb}$ (a), $^{13}\text{C} + ^{208}\text{Pb}$ (b), and $^{15}\text{C} + ^{208}\text{Pb}$ (c) at incident C energies of 54.07 MeV. The data in (a) and (b) are taken from [10]. The dotted curves denote the bare, no coupling calculations and the solid curves denote the results of the full calculations. The dashed curve in (b) denotes the result of a calculation with just the $^{208}\text{Pb}(^{13}\text{C},^{12}\text{C})$ transfer included and the dot-dashed curve in (c) denotes the result of a calculation assuming a $1d_{5/2}$ ground state for ^{15}C .

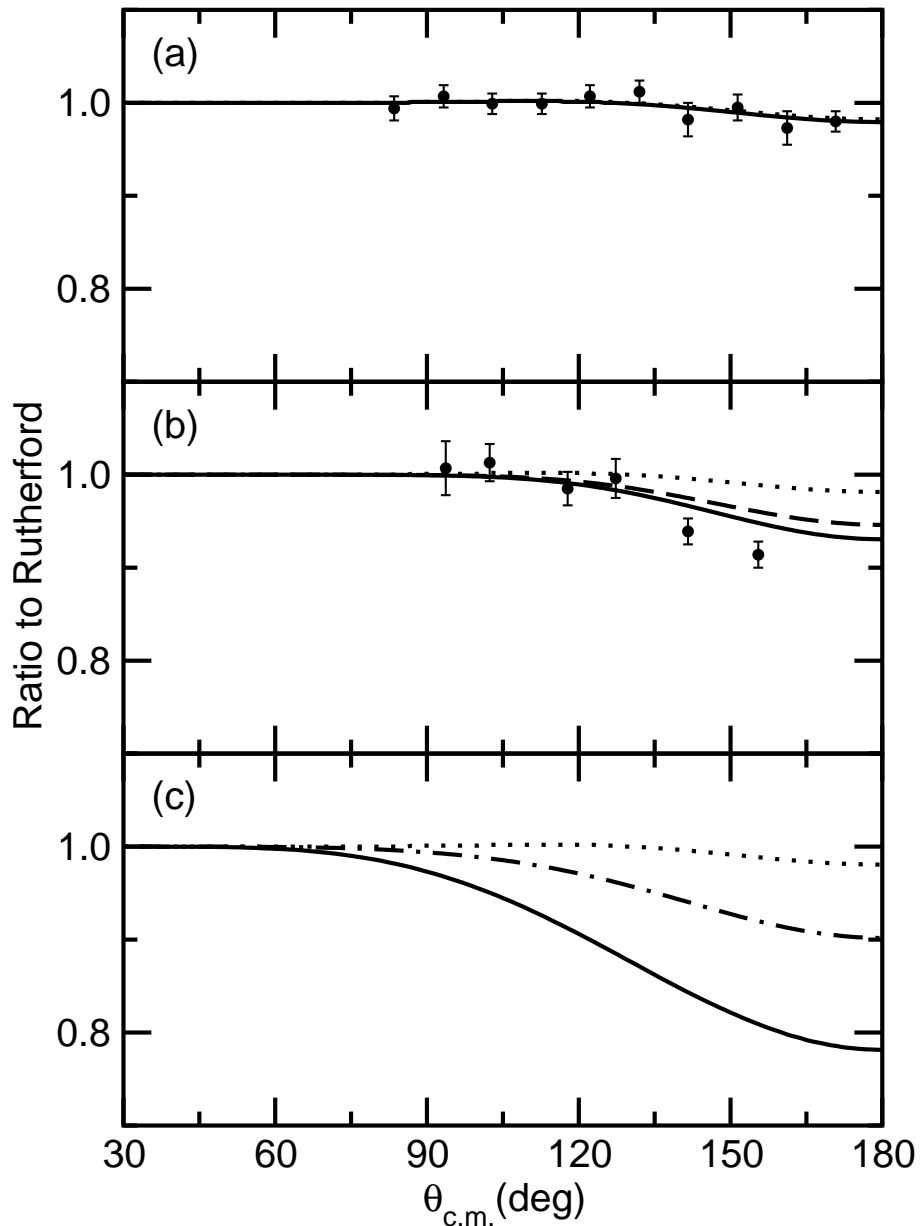
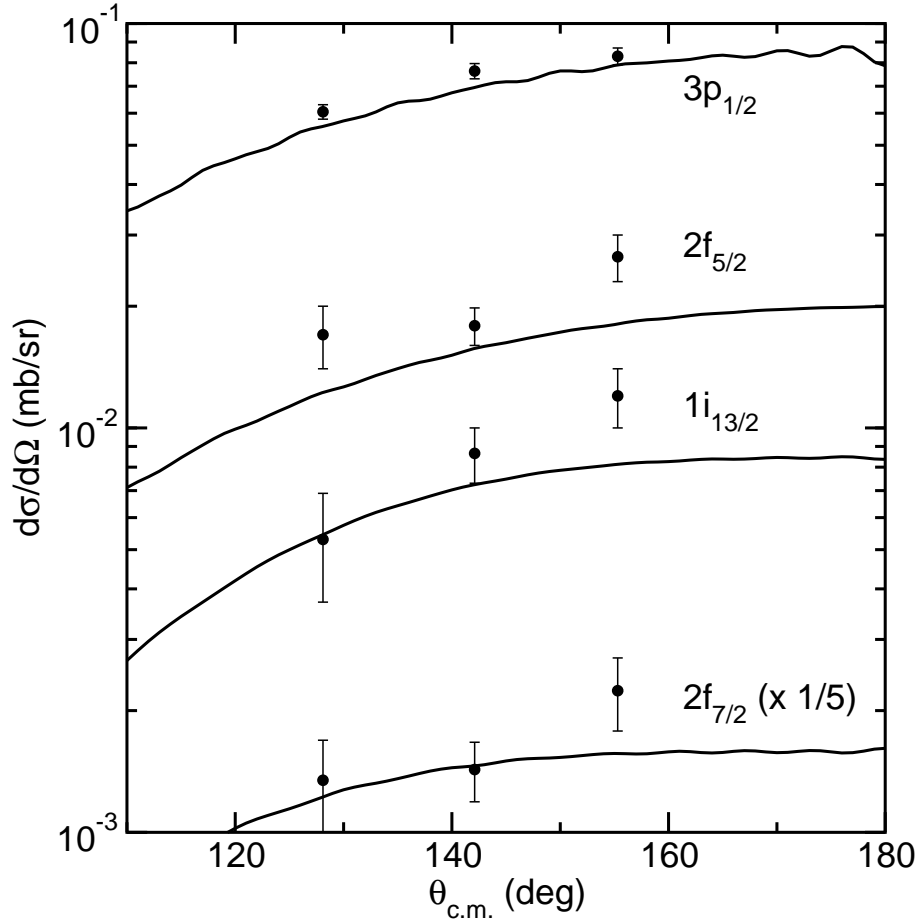


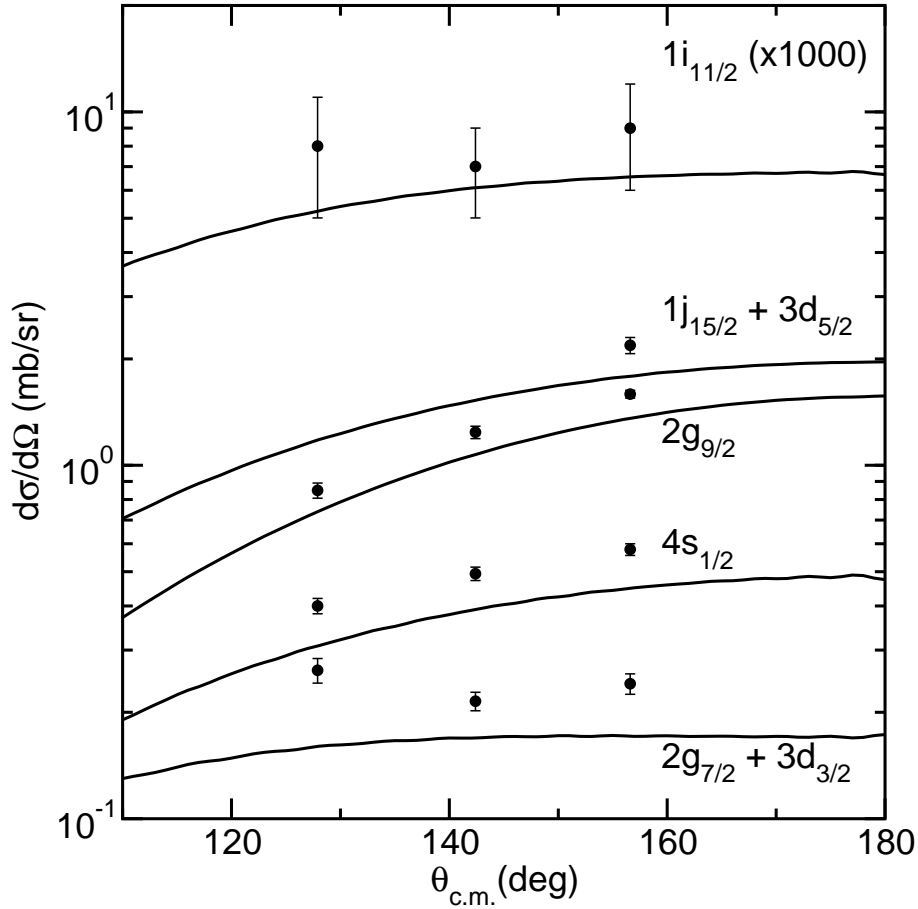
FIG. 2: Calculated $^{208}\text{Pb}(^{12}\text{C},^{13}\text{C})^{207}\text{Pb}$ angular distributions (solid curves) plus the data of [10] (filled circles) for an incident ^{12}C energy of 54.07 MeV.



small to be calculable, due to the very negative Q-value for this reaction (see Table I). In Fig. 2 we plot the calculated $^{208}\text{Pb}(^{12}\text{C},^{13}\text{C})^{207}\text{Pb}$ angular distributions together with the data of [10]. The agreement is satisfactory, validating our conclusions concerning the lack of effect of transfer coupling in this system at sub-barrier energies.

In Fig. 1(b) we see that coupling to single neutron transfer reactions has a small but significant effect on the $^{13}\text{C} + ^{208}\text{Pb}$ elastic scattering at this sub-barrier energy. In Figs. 3 and 4 we plot the calculated $^{208}\text{Pb}(^{13}\text{C},^{12}\text{C})^{209}\text{Pb}$ and $^{208}\text{Pb}(^{13}\text{C},^{14}\text{C})^{207}\text{Pb}$ angular distributions, respectively, together with the data of [10]. Agreement between calculation and data is again satisfactory, although the $^{208}\text{Pb}(^{13}\text{C},^{12}\text{C})^{209}\text{Pb}$ data are consistently under predicted while the elastic scattering data is somewhat over predicted at backward angles. This is due to our use of the shell model spectroscopic factor quoted in [12] for the $^{13}\text{C}:^{12}\text{C}$

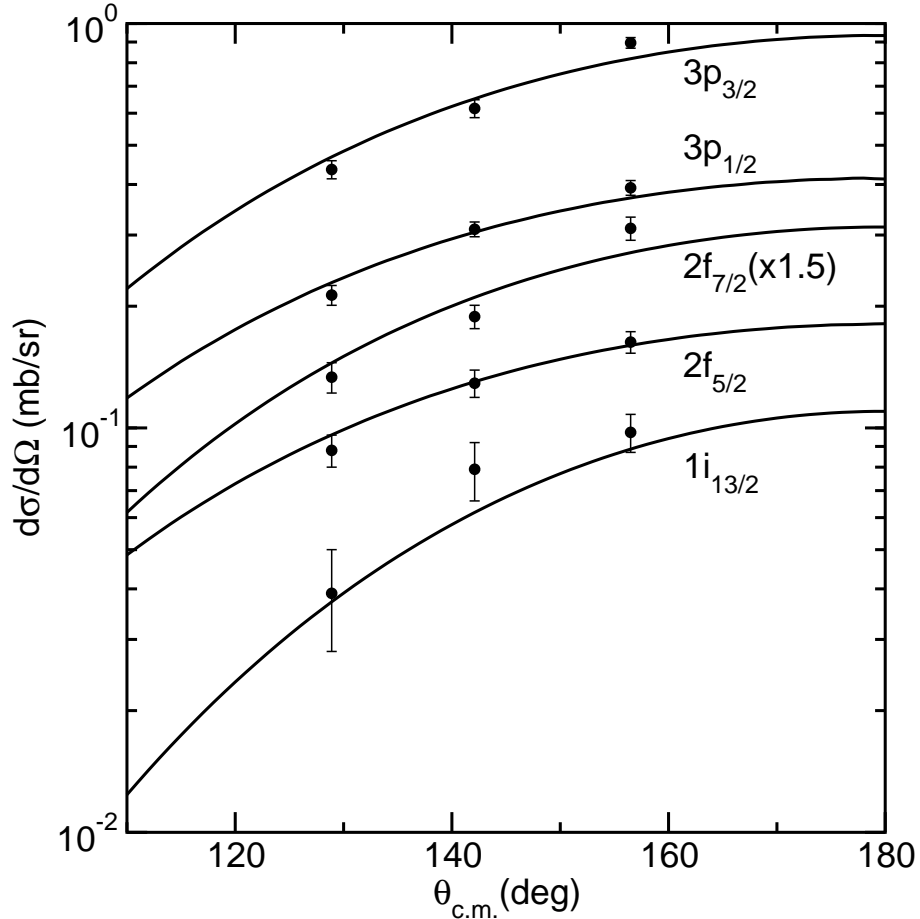
FIG. 3: Calculated $^{208}\text{Pb}(^{13}\text{C},^{12}\text{C})^{209}\text{Pb}$ angular distributions (solid curves) plus the data of [10] (filled circles) for an incident ^{13}C energy of 54.07 MeV.



overlap which is somewhat smaller (0.61) than the lower limit of the empirical value of 0.75 ± 0.1 [12]. Taking a value of 0.75 for this spectroscopic factor gives good agreement with the $^{208}\text{Pb}(^{13}\text{C},^{12}\text{C})^{209}\text{Pb}$ transfer data and improves the agreement with the elastic scattering (it is still slightly over predicted at backward angles). Similar remarks apply to the $^{208}\text{Pb}(^{12}\text{C},^{13}\text{C})^{207}\text{Pb}$ transfer, although the effect is less marked; the effect of the transfer coupling on the elastic scattering is so small in this case that the slight increase in spectroscopic factor has a negligible effect. We have nevertheless chosen to present the results using the shell model value as an example of the predictive power of such calculations when realistic structure information is employed as input.

Finally, in Fig. 1(c) we see that coupling to the $^{208}\text{Pb}(^{15}\text{C},^{14}\text{C})^{209}\text{Pb}$ single neutron stripping has a large effect on the elastic scattering at backward angles. The solid curve in Fig.

FIG. 4: Calculated $^{208}\text{Pb}(^{13}\text{C},^{14}\text{C})^{207}\text{Pb}$ angular distributions (solid curves) plus the data of [10] (filled circles) for an incident ^{13}C energy of 54.07 MeV.



1(c) does not include the $^{208}\text{Pb}(^{15}\text{C},^{16}\text{C})^{207}\text{Pb}$ coupling as tests found that it has a negligible effect on the elastic scattering at this energy. The test calculations included inelastic excitation of the 0.74 MeV $5/2^+$ first excited state of ^{15}C and transfer from this state to the ground state of ^{16}C in addition to the ground state to ground state transfer. The two step transfer path via the first excited state of ^{15}C was included as the spectroscopic factor for single neutron pickup to the ground state of ^{16}C via this state is twice that via the ground state of ^{15}C [13]. We used the $B(E2)$ value quoted in [18] and derived the necessary nuclear deformation length using the collective model and a radius of $1.2 \times 15^{1/3}$ fm; while this procedure may be questionable for a halo nucleus, it should be adequate for our purposes as the excitation is Coulomb dominated at the low incident energy considered here. The inelastic coupling itself has a small effect on the elastic scattering, insignificant in comparison to that

due to the $^{208}\text{Pb}(^{15}\text{C},^{14}\text{C})^{209}\text{Pb}$ transfer.

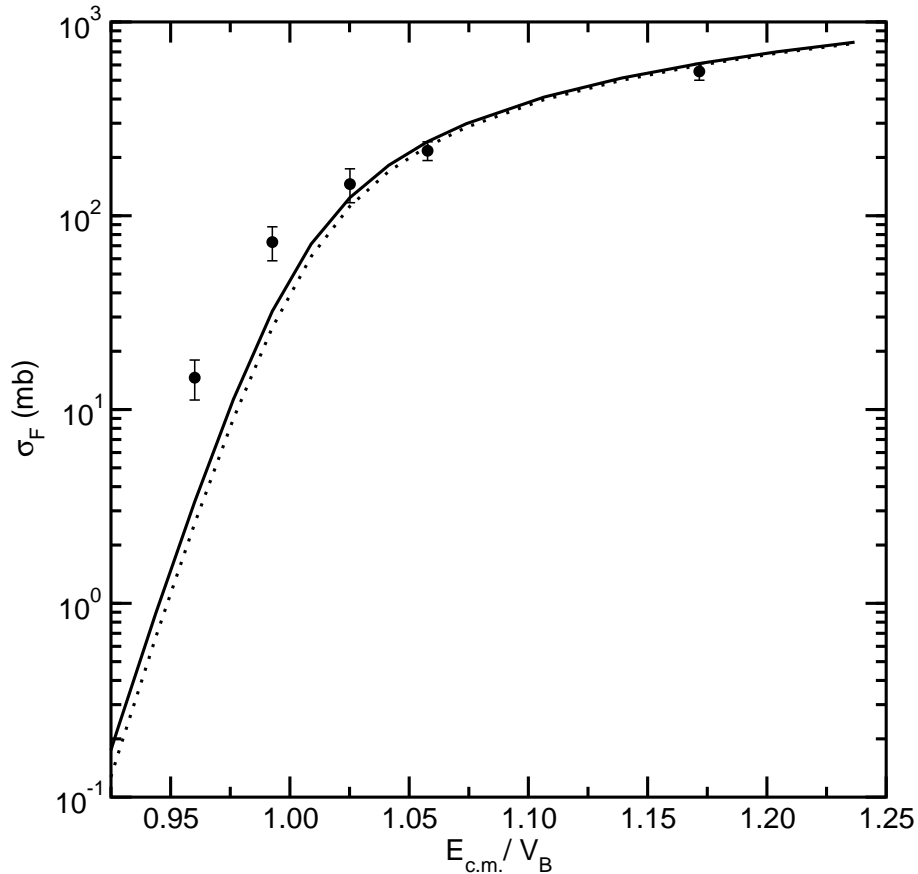
It is interesting to note that our naive *a priori* expectations concerning the effect of the transfer couplings in passing from ^{12}C to ^{15}C are not entirely justified by the results; although ^{13}C does indeed exhibit behavior intermediate between ^{12}C and ^{15}C it is the negative Q-value (-1.0 MeV) $^{208}\text{Pb}(^{13}\text{C},^{12}\text{C})^{209}\text{Pb}$ reaction that has the most important effect on the elastic scattering. As noted above, reaction Q-values are not the sole criteria for determining whether a given coupling will have a significant influence on the elastic scattering and they are often not the most important factor — virtual couplings to classically closed channels often prove to have significant effects on elastic scattering, see e.g. [19, 20].

The most striking result is the very large effect due to single neutron stripping on the $^{15}\text{C} + ^{208}\text{Pb}$ elastic scattering. This may be ascribed to the halo nature of ^{15}C ; the extended wave function of the valence neutron leads to larger transfer probabilities at large radii than for a “conventional” nucleus. We may illustrate this by a test calculation. The well-known inversion of the $2s_{1/2}$ and $1d_{5/2}$ levels in ^{15}C leads to a $1/2^+$ ground state for this nucleus, with the valence neutron in the $2s_{1/2}$ orbital. Even with the standard binding potential parameters that we have employed in our calculations, combined with the relatively low binding energy for the last neutron this will lead to a halo character for the ground state of ^{15}C and thus to enhanced transfer probability. The result of a test calculation assuming a $1d_{5/2}$ ground state is shown on Fig. 1(c) as the dot-dashed curve — it is apparent that the effect of the transfer coupling is much reduced, and is comparable with that for the $^{13}\text{C} + ^{208}\text{Pb}$ system.

Breakup may also play a rôle for ^{15}C , in contrast to ^{12}C and ^{13}C , due to the low threshold (1.22 MeV) against the $^{15}\text{C} \rightarrow n + ^{14}\text{C}$ process. Test calculations employing a simplistic $^{14}\text{C} + n$ model of ^{15}C with an inert ^{14}C core suggest that breakup coupling effects could be as large, if not larger, than those due to the $^{208}\text{Pb}(^{15}\text{C},^{14}\text{C})^{209}\text{Pb}$ transfer at sub-barrier energies. However, whatever the actual effect of breakup coupling may be, it does not affect the large contribution from single neutron stripping.

We have thus far been concerned with the effect of neutron transfer coupling on sub-barrier elastic scattering and found a large effect for the halo nucleus ^{15}C , in contrast to the two stable Carbon isotopes. However, as measurements of the total fusion excitation function for systems involving ^{15}C as the projectile are planned at several laboratories, we have also calculated the total fusion excitation functions for the three systems ^{12}C , ^{13}C and

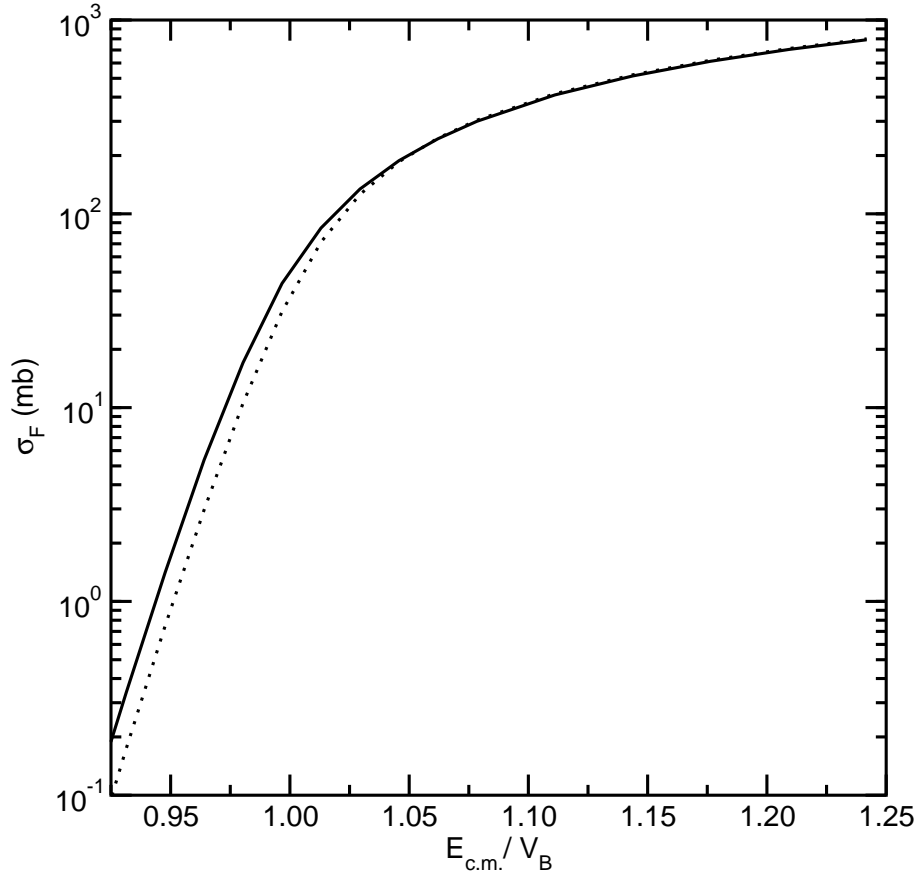
FIG. 5: Calculated $^{12}\text{C} + ^{208}\text{Pb}$ total fusion excitation functions with (solid curve) and without (dotted curve) the $^{208}\text{Pb}(^{12}\text{C},^{13}\text{C})^{209}\text{Pb}$ transfer coupling compared to the data of [21] (filled circles).



$^{15}\text{C} + ^{208}\text{Pb}$ to investigate whether the halo nature of ^{15}C also leads to new effects for this observable. The results are shown in Figs. 5-7. As for the elastic scattering, the calculations for the $^{12}\text{C} + ^{208}\text{Pb}$ system omit the $^{208}\text{Pb}(^{12}\text{C},^{11}\text{C})$ couplings and those for $^{15}\text{C} + ^{208}\text{Pb}$ omit the $^{208}\text{Pb}(^{15}\text{C},^{16}\text{C})$ couplings. The effect of the $^{208}\text{Pb}(^{12}\text{C},^{11}\text{C})$ couplings on the total fusion cross section was found to be negligible over the energy range studied, and while there was a small effect due to the $^{208}\text{Pb}(^{15}\text{C},^{16}\text{C})$ couplings this was found to be due mostly to the inelastic excitation of ^{15}C to its first excited state, included in the calculations.

We also show the measured total fusion cross sections for the $^{12}\text{C} + ^{208}\text{Pb}$ system of [21] in Fig. 5 for comparison. At above barrier incident energies where coupling effects are expected to be small there is good agreement between the calculated and measured cross sections for this system. At sub-barrier energies the calculations considerably under

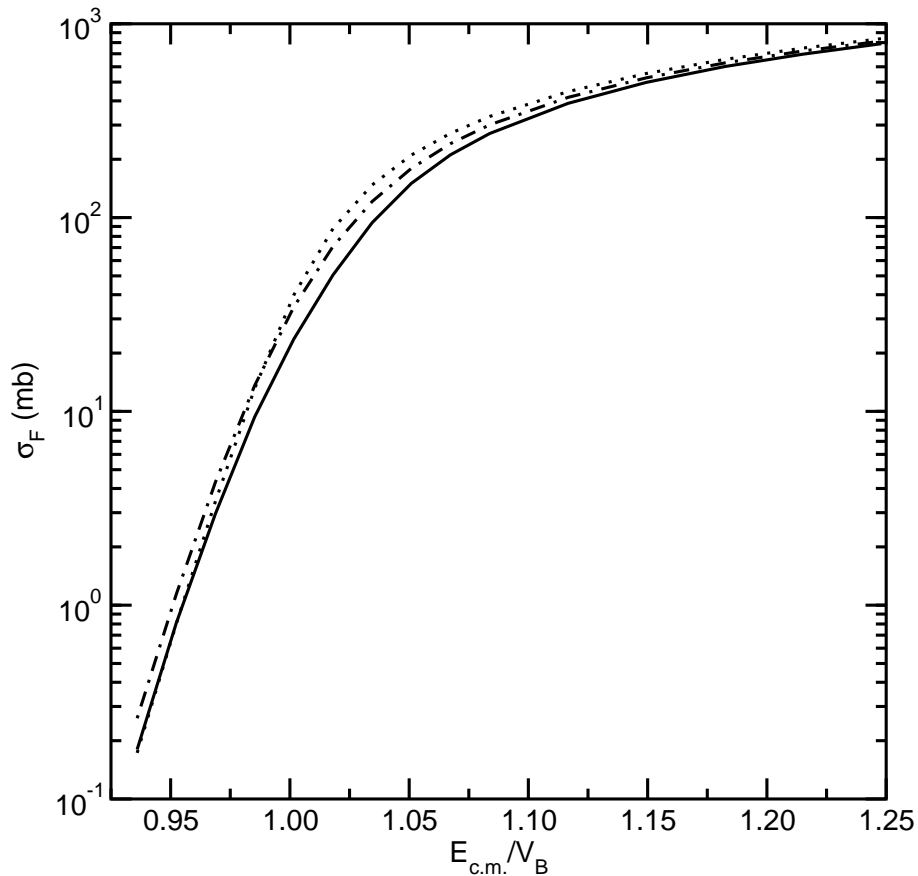
FIG. 6: Calculated $^{13}\text{C} + ^{208}\text{Pb}$ total fusion excitation functions with (solid curve) and without (dotted curve) the $^{208}\text{Pb}(^{13}\text{C}, ^{12}\text{C})^{209}\text{Pb}$ and $^{208}\text{Pb}(^{13}\text{C}, ^{14}\text{C})^{207}\text{Pb}$ transfer couplings.



estimate the data; this may be ascribed to the neglect of couplings to inelastic excitations of the target and projectile, as tests confirm that while these couplings have a negligible effect on the elastic scattering at sub-barrier energies they give rise to a considerable enhancement of the fusion cross section. Indeed, more complete calculations presented in [21] that include these couplings are able to well describe the fusion data.

We see trends in the coupling effects on the total fusion cross section as we pass from ^{12}C to ^{15}C that are in some ways similar to those for the elastic scattering; the single neutron stripping has little effect on the total fusion cross section for the $^{12}\text{C} + ^{208}\text{Pb}$ system while for $^{13}\text{C} + ^{208}\text{Pb}$ we see a significant near and sub-barrier enhancement due to the nucleon transfer couplings. In the $^{15}\text{C} + ^{208}\text{Pb}$ system the $^{208}\text{Pb}(^{15}\text{C}, ^{14}\text{C})$ couplings have a negligible effect on the sub-barrier total fusion cross section. Thus, in the sub-barrier regime single neutron transfers have the greatest influence on the total fusion cross section for the ^{13}C

FIG. 7: Calculated $^{15}\text{C} + ^{208}\text{Pb}$ total fusion excitation functions with (solid curve) and without (dotted curve) the $^{208}\text{Pb}(^{15}\text{C}, ^{14}\text{C})^{209}\text{Pb}$ transfer coupling. The dot-dashed curve denotes the result of a calculation including the transfer coupling but assuming a $1d_{5/2}$ ground state for ^{15}C .



$+ ^{208}\text{Pb}$ system, in contrast to the situation for the elastic scattering. However, in the $^{15}\text{C} + ^{208}\text{Pb}$ system we find that for incident energies just above the barrier the single neutron stripping coupling has an important effect on the total fusion cross section not seen in the other two systems studied here, viz, a significant hindrance of the cross section compared to the no-coupling case. This appears to be a general phenomenon for halo systems, and has been demonstrated for a number of these nuclei, see [22].

We also performed test calculations of the total fusion for the $^{13}\text{C} + ^{208}\text{Pb}$ system where the $^{208}\text{Pb}(^{13}\text{C}, ^{12}\text{C})^{209}\text{Pb}$ coupling was omitted. The resulting excitation function was indistinguishable from that of the full calculation on a plot, leading us to conclude that the $^{208}\text{Pb}(^{13}\text{C}, ^{12}\text{C})^{209}\text{Pb}$ coupling has no significant influence on the total fusion cross section in the sub and near-barrier energy regime. This is in contrast to the sub-barrier elastic scatter-

ing where this coupling is the most important and the influence of the $^{208}\text{Pb}(^{13}\text{C},^{14}\text{C})^{207}\text{Pb}$ coupling is weak.

A further series of test calculations investigated the effect of assuming a $1d_{5/2}$ configuration for the “valence” neutron in the ground state of ^{15}C . The results are plotted as the dot-dashed curve in Fig. 7. The effect of the $^{208}\text{Pb}(^{15}\text{C},^{14}\text{C})^{209}\text{Pb}$ coupling is now much closer to that found for conventional nuclei, in that we now see a sub-barrier enhancement due to coupling while the above barrier hindrance is much reduced. We again see the importance of the $2s_{1/2}$ configuration for the halo in ^{15}C , as for the sub-barrier elastic scattering.

To summarize, we have performed a series of coupled reaction channels calculations investigating the effect of single neutron transfer couplings on the sub-barrier elastic scattering and near barrier total fusion of ^{12}C , ^{13}C and $^{15}\text{C} + ^{208}\text{Pb}$. A satisfactory description of the available elastic scattering and transfer data for the ^{12}C and $^{13}\text{C} + ^{208}\text{Pb}$ systems was obtained with no adjustable parameters. We found an evolution in the importance of the coupling effect on the elastic scattering in passing from ^{12}C (no effect) to ^{15}C (large effect), with ^{13}C exhibiting intermediate behavior. The large effect for ^{15}C was shown to be due to the halo nature of this isotope, linked to the dominant $2s_{1/2}$ structure of the ground state. The evolution of the coupling effects on the near barrier total fusion excitation functions was more complex, the largest effect in the sub-barrier regime being found in the $^{13}\text{C} + ^{208}\text{Pb}$ system, while in the $^{15}\text{C} + ^{208}\text{Pb}$ system a significant hindrance of the total fusion cross section at incident energies just above the barrier due to the single neutron stripping coupling was found. This latter effect has been observed in other systems involving halo projectiles [22] and seems to be characteristic of these nuclei. The effect was again found to be linked to the dominant $2s_{1/2}$ structure of the ground state in ^{15}C . We therefore find that the halo nature of the ^{15}C ground state is predominantly due to its $2s_{1/2}$ structure rather than the weak binding of the valence neutron; although the latter does play a rôle it is not sufficient by itself to produce the full halo-like effect on either the elastic scattering or the total fusion, as the test calculations assuming a $1d_{5/2}$ configuration show.

Acknowledgments

The authors would like to thank Dr. A. Shrivastava for supplying the $^{12}\text{C} + ^{208}\text{Pb}$ fusion excitation function data in tabular form. N.K. gratefully acknowledges the receipt of a Marie

- [1] O. R. Kakuee, J. Rahighi, A. M. Sanchez-Benitez, M. V. Andres, S. Cherubini, T. Davinson, W. Galster, J. Gómez-Camacho, A. M. Laird, M. Laméhi-Rachti, I. Martel, A. C. Shotter, W. B. Smith, J. Vervier, and P. J. Woods, *Nucl. Phys.* **A728**, 339 (2003).
- [2] O. R. Kakuee, M. A. G. Alvarez, M. V. Andres, S. Cherubini, T. Davinson, A. Di Pietro, W. Galster, J. Gómez-Camacho, A. M. Laird, M. Laméhi-Rachti, I. Martel, A. M. Moro, J. Rahighi, A. M. Sanchez-Benitez, A. C. Shotter, W. B. Smith, J. Vervier, P. J. Woods, *Nucl. Phys.* **A765**, 294 (2006).
- [3] A. Di Pietro, P. Figuera, F. Amorini, C. Angulo, G. Cardella, S. Cherubini, T. Davinson, D. Leanza, J. Lu, H. Mahmud, M. Milin, A. Musumarra, A. Ninane, M. Papa, M. G. Pellegriti, R. Raabe, F. Rizzo, C. Ruiz, A. C. Shotter, N. Soic, S. Tudisco, and L. Weissman, *Phys. Rev. C* **69**, 044613 (2004).
- [4] K. Rusek, N. Keeley, K. W. Kemper, and R. Raabe, *Phys. Rev. C* **67**, 041604 (2003).
- [5] N. Keeley, J. M. Cook, K. W. Kemper, B. T. Roeder, W. D. Weintraub, F. Maréchal, and K. Rusek, *Phys. Rev. C* **68**, 054601 (2003).
- [6] K. Rusek, I. Martel, J. Gómez-Camacho, A. M. Moro, and R. Raabe, *Phys. Rev. C* **72**, 037603 (2005).
- [7] T. Matsumoto, T. Egami, K. Ogata, Y. Iseri, M. Kamimura, and M. Yahiro, *Phys. Rev. C* **73**, 051602 (2006).
- [8] J. P. Bychowski, P. A. DeYoung, B. B. Hilldore, J. D. Hinnefeld, A. Vida, F. D. Becchetti, J. Lupton, T. W. O'Donnell, J. J. Kolata, G. Rogachev, and M. Hencheck, *Phys. Lett.* **B596**, 26 (2004).
- [9] P. A. DeYoung, P. J. Mears, J. J. Kolata, E. F. Aguilera, F. D. Becchetti, Y. Chen, M. Cloughesy, H. Griffin, C. Guess, J. D. Hinnefeld, H. Jiang, S. R. Jones, U. Khadka, D. Lizcano, E. Martinez-Quiroz, M. Ojaniega, G. F. Peaslee, A. Pena, J. Rieth, S. VanDenDriessche, and J. A. Zimmermann, *Phys. Rev. C* **71**, 051601(R) (2005).
- [10] M. A. Franey, J. S. Lilley, and W. R. Phillips, *Nucl. Phys.* **A324**, 193 (1979).
- [11] T. Aumann, *Eur. Phys. J. A* **26**, 441 (2005).

- [12] M. B. Tsang, J. Lee, and W. G. Lynch, *Phys. Rev. Lett.* **95**, 222501 (2005).
- [13] V. Maddalena, T. Aumann, D. Bazin, B. A. Brown, J. A. Caggiano, B. Davids, T. Glasmacher, P. G. Hansen, R. W. Ibbotson, A. Navin, B. V. Pritychenko, H. Scheit, B. M. Sherrill, M. Steiner, J. A. Tostevin, and J. Yurkon, *Phys. Rev. C* **63**, 024613 (2001).
- [14] D. G. Kovar, N. Stein, and C. K. Bockelman, *Nucl. Phys.* **A231**, 266 (1974).
- [15] R. A. Broglia and A. Winther, *Heavy Ion Reactions*, (Benjamin/Cummings, New York, 1981), Vol. 1, p. 114.
- [16] M. J. Rhoades-Brown and P. Braun-Munzinger, *Phys. Lett.* **B136**, 19 (1984).
- [17] I. J. Thompson, *Comput. Phys. Rep.* **7**, 167 (1988).
- [18] Y. Suzuki, H. Matsumura, and B. Abu-Ibrahim, *Phys. Rev. C* **70**, 051302(R) (2004).
- [19] I. J. Thompson, M. A. Nagarajan, J. S. Lilley, and M. J. Smithson, *Nucl. Phys.* **A505**, 84 (1989).
- [20] N. Keeley, J. S. Lilley, and J. A. Christley, *Nucl. Phys.* **A603**, 97 (1996).
- [21] S. Santra, P. Singh, S.Kailas, A. Chatterjee, A. Shrivastava, and K. Mahata, *Phys. Rev. C* **64** 024602 (2001).
- [22] N. Keeley, R. Raabe, N. Alamanos, and J.-L. Sida, *Prog. Part. Nucl. Phys.*, in press. arXiv:nucl-ex/0702038.